J. Acoust. Soc. Jpn. (*E*) **21**, 2 (2000)

PAPER

Basic characteristics and accuracy of acoustic element using spline function in finite element sound field analysis

Toru Otsuru and Reiji Tomiku

Faculty of Engineering, Oita University, 700, Dannoharu, Oita, 870-1192 Japan

(*Received 5 April 1999*)

A 27-node isoparametric acoustic element, namely Spl 27, using the spline interpolation polynomials for the analysis of sound fields in rooms is presented first. Next, the basic characteristics of the element are discussed by comparing with the conventional elements in the eigenanalysis of a small room. Then, the mechanism of causing errors in eigenanalysis is investigated to propose error-characteristic curves as proper guidelines for the appropriate applications of the elements. An example application on a three dimensional sound field proved that, if the size of elements satisfies the value given by the guideline, Spl 27 can be expected to provide both fair eigenfrequency approximation within 1% relative error and exact modal order agreement with the analytic solution. Finally, its application to a one-dimensional sound field proved that the guideline estimated by the error-characteristic curves give satisfactory results in the approximation of sound pressure waveforms. The basic relation between the eigenmode approximation and resulting sound pressure response was clarified through the process.

Keywords: Finite-element-method, Interpolation-polynomial, Eigenvalue, Spline-polynomial, Accuracy-estimation

PACS number: 43. 55. Ka

1. INTRODUCTION

Numerical methods have been intensively used to analyze acoustic problems of many kinds. The finite element method (FEM) is advantageous in its broad range of adaptability among the numerical methods based on the wave equation especially when the sound fields in closed cavities are being investigated. Although many works have been done on and around acoustic problems using the FEM, it is necessary to prove the basic relation between the properties of elements and the resulting accuracy. It is especially the case in the sound field analysis on architectural acoustics because huge amounts of degrees of freedom would usually be required ; when a proper estimation about the cost-effectiveness would be of great importance. In this paper, a 27-node acoustic element using spline polynomials is proposed first. Then, the following basic investigations reveal the systematic relation among element division, the accuracy of eigen-analysis of a room and the resulting sound pressure in a simple sound field.

2. FORMULATION OF 27-NODE ISOPARAMETRIC ACOUSTIC FINITE ELEMENT

The 8- and 20-node elements are widely used in many works on the analysis of three-dimensional sound field from the early decade of the FEM.[1-4] While, elements build up on 27-node are advantageous because their nodal locations can directly be applied to analysis by 8-node elements.

2.1 Formulation of Element Matrices

Following the standard finite elemental proce-

dure, the acoustic element matrices are given as follows; first let the sound pressure, p, at an arbitrary point in an element be expressed by

$$P=\{N\}^{\mathrm{T}}\{p\}_e . \tag{1}$$

The kinetic and potential energy in an element can be derived for the angular frequency of ω by,

$$T_e=\frac{1}{2}\left(\frac{1}{\rho\omega^2}\right)\iiint_c\left\{\left(\frac{\partial p}{\partial x}\right)^2+\left(\frac{\partial p}{\partial y}\right)^2+\left(\frac{\partial p}{\partial z}\right)^2\right\}dxdydz \tag{2}$$

$$V_e=\frac{1}{2}\left(\frac{1}{\rho c^2}\right)\iiint_e p^2\,dxdydz . \tag{3}$$

The work done by the external force is,

$$W_e=\int_{\Gamma_e} u_n p\,dl_e . \tag{4}$$

With them, by applying Hamilton's principle to the Lagrangian of the system, the following discrete formula can be obtained;

$$([K]_e-\omega^2[M]_e)\{p\}_e=\rho\omega^2\{u\}_e . \tag{5}$$

The matrices used here, $[K]_e$ and $[M]_e$, are defined by

$$[K]_e=\iiint_e\left[\frac{\partial\{N\}}{\partial x}\ \frac{\partial\{N\}}{\partial y}\ \frac{\partial\{N\}}{\partial z}\right]\cdot\left[\frac{\partial\{N\}}{\partial x}\ \frac{\partial\{N\}}{\partial y}\ \frac{\partial\{N\}}{\partial z}\right]^{\mathrm{T}}dxdydz . \tag{6}$$

$$[M]_e=\frac{1}{c^2}\iiint_e\{N\}\{N\}^{\mathrm{T}}dxdydz . \tag{7}$$

The global matrices and global matrix equation can be assembled with these elemental matrices, and the global matrix equation can be written by

$$([K]-\omega^2[M])\{p\}=\rho\omega^2\{u\} . \tag{8}$$

The eigenvalue, ω_n^2, and the eigenvector, $\{\phi_n\}$, can be obtained by solving

$$([K]-\omega_n^2[M])\{\phi_n\}=0 . \tag{9}$$

2.2 Shape Functions

Figure 1 shows the nodal points in a three-dimensional 27-node finite element. To construct shape functions of the elements, Lagrange and spline interpolation polynomials can be employed as below.

With the given values $f(\xi_i)$ at the nodal points ξ_i ($i=1, 2, \ldots, \nu$), a function $P(\xi)$ can be interpolated by

$$P(\xi)=\sum_{i=1}^{\nu} f(\xi_i)L_i(\xi) . \tag{10}$$

Here Lagrange interpolation polynomials are given by

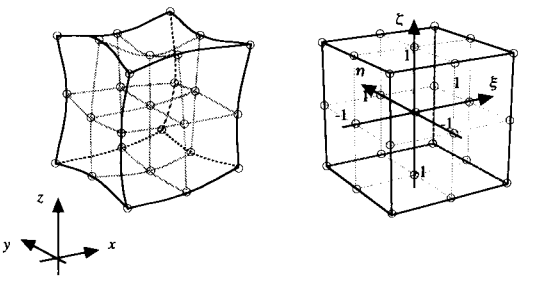

Fig. 1 27-Node acoustic element (a) in global co-ordinate of (x, y, z), and (b) in local co-ordinate of (ξ, η, ζ).

$$L_i(\xi)=\prod_{\substack{j=1\\(j\neq i)}}^{\nu}\frac{\xi-\xi_j}{\xi_i-\xi_j} . \tag{11}$$

To construct the shape function for the element shown in Fig. 1, the following polynomials can be applied.

$$L_1(\xi)=\prod_{\substack{j=1\\(j\neq 1)}}^{3}\frac{\xi-\xi_j}{\xi_1-\xi_j}=\frac{\xi(\xi-1)}{2} , \tag{12}$$

$$L_2(\xi)=(1-\xi^2) , \tag{13}$$

$$L_3(\xi)=\frac{\xi(\xi+1)}{2} . \tag{14}$$

There, at the three points ($\xi_1=-1$, $\xi_2=0$, $\xi_3=1$),

$L_1(\xi_1)=1$, $L_1(\xi_2)=0$, $L_1(\xi_3)=0$: for Eq.(12)
$L_2(\xi_1)=0$, $L_2(\xi_2)=1$, $L_2(\xi_3)=0$: for Eq.(13)
$L_3(\xi_1)=0$, $L_3(\xi_2)=0$, $L_3(\xi_3)=1$: for Eq.(14)

are assumed.

While, the authors tried to apply the cubic spline $S_i(\xi)$ with the same number of nodal points as Lagrange polynomials.

$$S_i(\xi)=f(\xi_i)+c_{i1}(\xi-\xi_i)+c_{i2}(\xi-\xi_i)^2+c_{i3}(\xi-\xi_i)^3 \qquad \xi_1\leq\xi\leq\xi_{i+1},\quad i=1,2,\ldots,\nu \tag{15}$$

For simplicity, let us employ the natural cubic spline which assumes that $\partial^2 S_i/\partial\xi^2$ at both ends of an interval zero.[5] Then the coefficients c_{i1}, c_{i2} and c_{i3} can be defined and the final form of polynomials can be written as follows:

$$P(\xi)=\sum_{i=1}^{3} f(\xi_i)S_i(\xi) \tag{16}$$

$$S_1(\xi)=\begin{cases}0.25\xi^3+0.75\xi^2-0.5\xi : \xi\in[-1, 0]\\ -0.25\xi^3+0.75\xi^2-0.5\xi : \xi\in[0, 1]\end{cases} \tag{17}$$

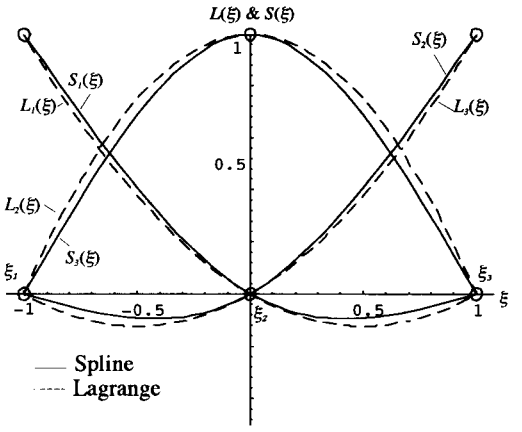

Fig. 2 Comparison of Lagrange and spline polynomials.

$$S_2(\xi)=\begin{cases}-0.5\xi^3-1.5\xi^2+1 : \xi\in[-1,0]\\ 0.5\xi^3-1.5\xi^2+1 : \xi\in[0,1]\end{cases} \tag{18}$$

$$S_3(\xi)=\begin{cases}0.25\xi^3+0.75\xi^2+0.5\xi : \xi\in[-1,0]\\ -0.25\xi^3+0.75\xi^2+0.5\xi : \xi\in[0,1]\end{cases} \tag{19}$$

The basic shapes of Lagrange and spline polynomials are compared in Fig. 2. Although the difference of the two functions seems to be small, their characteristics differ considerably a lot in the investigation on the accuracy of eigenanalysis in the following sections.

With these polynomials, shape functions for 27-node elements can be defined as follows:

$$\{N\}=\{N_1, N_2, N_3,\ldots,N_{27}\}\,. \tag{20}$$

Here, $N_m=L_iL_jL_k$ for the Lagrange element and $N_m=S_iS_jS_k$ for the spline element, and i, j and k correspond to the nodal order in ξ-, η-, and ζ-direction of the elemental node m respectively, ($m=1, 2, \ldots, 27$).

In addition, though these shape functions are constructed on the local co-ordinate of (ξ,η,ζ), the matrices in the Equations (6) and (7), which are on the global co-ordinate of (x,y,z), can be obtained using the Jacobean matrix.

3. COMPARISON OF EIGENMODE APPROXIMATION AMONG ELEMENTS

The eigenanalysis on a rectangular room with the dimension of $1.56\times0.72\times0.54\,[m^3]$ are carried out to compare the accuracy among four element types:

Table 1 Number of elements and degrees of freedom used in the eigenanalysis.

Element type	Division (l_x, l_y, l_z)	Degrees of freedom
Lin 8	(2, 2, 2)	27
Ser 20	(2, 1, 1)	32
Lag 27	(1, 1, 1)	27
Spl 27	(1, 1, 1)	27

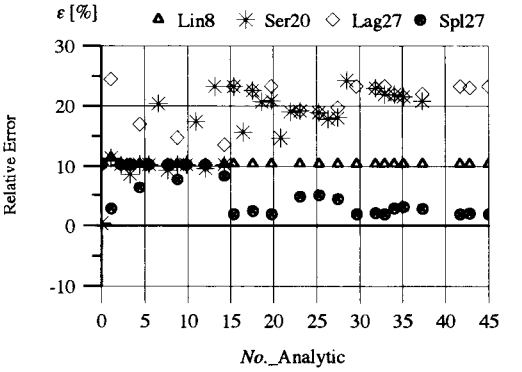

Fig. 3 Comparison of relative errors in eigenanalysis computed by FEM using four element types.

hexahedron 8-node isoparametric linear element[6] (Lin 8), hexahedron 20-node isoparametric serendipity element[6] (Ser 20), hexahedron 27-node isoparametric Lagrange element (Lag 27) and hexahedron 27-node isoparametric spline element (Spl 27). Both the arrays of element division, (l_x, l_y, l_z), and the degrees of freedom used in the eigenanalysis are given in Table 1, which shows the same degrees of freedom are used in Lin 8, Lag 27 and Spl 27, while about 20% higher degrees of freedom are used in Ser 20.

Figure 3 shows the result of the eigenanalysis, where *No._*Analytic denotes the sequential number in order of natural frequency, f_n, obtained by the analytic solution using Equation (21).

$$f_n=\frac{c}{2}\sqrt{\left(\frac{n_x}{L_x}\right)^2+\left(\frac{n_y}{L_y}\right)^2+\left(\frac{n_z}{L_z}\right)^2}\,. \tag{21}$$

The relation between *No._*Analytic and the array of spatial mode order, (n_x, n_y, n_z), is easy to be found in the analytic solution. On the other hand, the numeric results of the Equation (9), eigenfrequencies and eigenvectors, do not give direct infor-

Table 2 Correspondence of eigenfrequencies obtained by analytic solution and by FEM with the four element types.

No._Analytic	Order (n_x, n_y, n_z)	Eigenfrequency [Hz] obtained by				
		Analytic	Lin 8	Ser 20	Lag 27	Spl 27
1	(0, 0, 0)	0	0	0	0	0
2	(1, 0, 0)	109	120	109	120	120
3	(2, 0, 0)	218	241	240	269	222
4	(0, 1, 0)	224	247	247	247	247
5	(1, 1, 0)	249	275	270	275	275
6	(2, 1, 0)	312	345	345	365	332
7	(0, 0, 1)	315	347	347	347	347
8	(3, 0, 0)	327	N/A	394	N/A	N/A
9	(1, 0, 1)	333	368	364	368	368
10	(2, 0, 1)	383	422	422	439	412
11	(0, 1, 1)	386	426	426	426	426
12	(3, 1, 0)	396	N/A	465	N/A	N/A
13	(1, 1, 1)	401	443	440	443	443
14	(4, 0, 0)	436	N/A	538	N/A	N/A
15	(2, 1, 1)	444	489	489	504	480
16	(0, 2, 0)	447	494	552	552	456
•	•	•	•	•	•	•

mation about the spatial mode orders, and they only give a sequential order. Therefore it is necessary to identify the relation between spatial mode orders and sequential orders, and the identification was carried out both computationally and graphically. In the computational confirmation the mode checker[7] was applied, and its results agreed with those obtained by graphically, or by drawing the contours of three dimensional sound pressure distribution. As for the analytic solution, all the modes up to 5 kHz were lined up, while those by FEM are restricted within the degrees of freedom allocated in their computations. Consequently, several blanks can be found in the mode orders in the data obtained by FEM : some examples of the correspondence are listed in Table 2.

In the Fig. 3, Spl 27 gives the best approximation to the analytic values. Here, the relative errors, ε, is defined by

$$\varepsilon=\frac{f_{n,\,\mathrm{FEM}}-f_{n,\,\mathrm{Analytic}}}{f_{n,\,\mathrm{Analytic}}}\times 100\,[\%]\,, \tag{22}$$

and, $f_{n,\mathrm{FEM}}$ and $f_{n,\mathrm{Analytic}}$ denote eigenfrequencies of nth mode obtained by FEM and analytic solution respectively. Figure 3 shows that most of the ε of Spl 27 are below 5% and they are small compared to those of the other three elements. In addition, it is interesting to compare those of Lag 27 with Spl 27 ; though not much difference can be found in their polynomial shapes shown in Fig. 2, the relative errors of Lag 27 are more than twice those of Spl 27.

4. MECHANISM OF CAUSING ERRORS IN EIGENMODE APPROXIMATION

In order to find the mechanism that causes the approximation errors in eigenanalysis, another eigenanalysis on a one-dimensional sound field with the length of 1 [m] was carried out. The elements applied were Lin 8, Lag 27 and Spl 27. The arrays of element divisions applied here were chosen to examine only the characteristics in the tube's longitudinal direction.

Figure 4 shows the error characteristics curves of eigenfrequency approximation by the three elements. Regardless of elemental divisions, clear relationship can be seen between the error, ε, and the ratio of λ/d ; here, λ and d denote acoustic wavelength and the nodal distance in an element respectively.

As for Lin 8, the ε is less than or equal to 20% throughout the region $\lambda/d\geq 2$. The ε gradually decreases as λ/d increases in the region $\lambda/d>2.5$. On the other hand, for Spl 27, the absolute value of ε is less and about 2% in the region $\lambda/d>4$; and at $\lambda/d=4$, the ε becomes about 10%. It is remarkable that small and stable errors within 1% can be seen throughout the region $\lambda/d>4.4$. Note that intermediate characteristics between these two elements

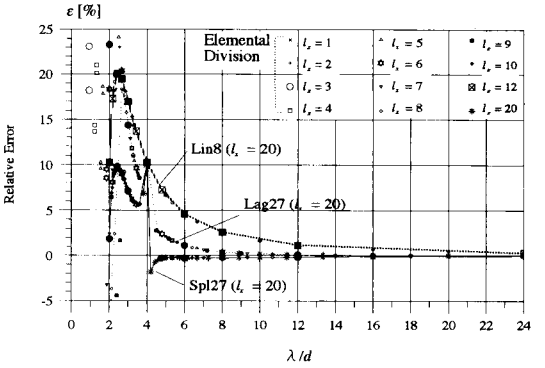

Fig. 4 Relation between modal order and relative errors in eigenanalysis by Lin 8, Spl 27 and Lag 27. Symbols denote spatial divisions.

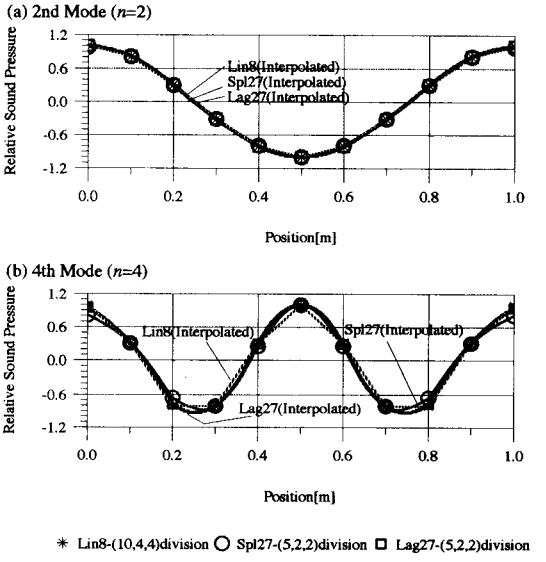

Fig. 5 Approximation of eigenmodes in "$\lambda/d>4$" by Lin 8, Lag 27 and Spl 27. (a) $n=2$, $\lambda/d=10$, (b) $n=4$, $\lambda/d=5$.

can be seen on Lag 27.

Mode shapes obtained through the eigenanalysis are shown in Fig. 5. Each symbol denotes discrete nodal values of sound pressure of the 2nd ($n=2$) and 4th ($n=4$) modes, and interpolated mode shapes are also given there as lines. Not much difference can be seen among the element types.

In the same manner, the shapes of 5th ($n=5$) modes are given in Fig. 6. All the values obtained by the three element types are located on the same line, which results in the same interpolated sawtooth

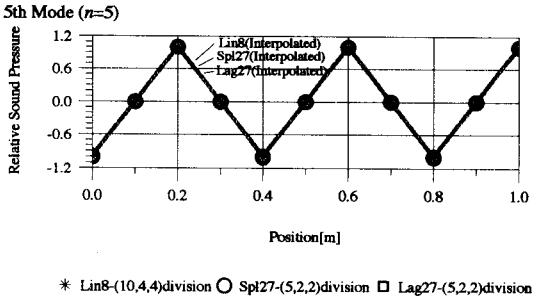

Fig. 6 Approximation of eigenmodes at "$\lambda/d=4$" by Lin 8, Lag 27 and Spl 27. $n=5$, $\lambda/d=4$.

wave. This is the reason that when $\lambda/d=4$, the relative errors in eigenfrequency computation of the three element types become the same value, *i.e.* 10%, as is shown in Fig. 4. Thus, on the condition that $\lambda/d>4$, successful interpolation of peaks in mode shapes assures small errors in the eigenfrequency approximation. The errors can be estimated referring to Fig. 4, and for 27-node elements half of λ/d gives the required number of elements per acoustic wavelength.

5. VERIFICATION OF THE MECHANISM

Several example eigenanalysis using both Spl 27 and Lin 8 were carried out on a three-dimensional room, $0.75\times0.53\times0.30$ [m^3]. The boundary conditions of the room were assumed to be hard. The arrays of element divisions applied were (6, 5, 5), (7, 5, 3), (4, 4, 2) and (3, 2, 1), and the same arrays of element divisions were given to both Lin 8 and Spl 27. The relative errors, ε, in the eigenanalysis are shown in Fig. 7 and Fig. 8 to compare the difference among the divisions. There, the modes are lined up in a simple sequence of frequency orders obtained through the numerical computations, which means that the modes with the same f_n do not always have the same array of spatial mode order ; and the following characteristics were found.

As for Spl 27, clear increases of relative errors can be found for all the spatial divisions. The numbers of orders at which the increases occur are listed in Table 3 named as N_0 with their spatial orders (n_x, n_y, n_z). Note that one of the three numbers otherwise 0 coincides with the number in the corresponding directions of element spatial divisions. The agreements of the mode shapes obtained by FEM

Table 3 Correspondence of element types, element division (l_x, l_y, l_z), critical order N_0, spatial mode order (n_x, n_y, n_z) and ε of N_0th and (N_0-1)th modes.

element type	division (l_x, l_y, l_z)	order N_0	(n_x, n_y, n_z) of Analytic Solution	ε [%] of N_0th mode	ε [%]of (N_0-1)th mode
Spl 27	(6, 5, 5)	59	(6, 0, 0)	1.13	−0.24
Spl 27	(7, 5, 3)	80	(0, 5, 0)	0.33	−0.28
Spl 27	(4, 4, 2)	21	(4, 0, 0)	1.55	−0.27
Spl 27	(3, 2, 1)	9	(0, 2, 0)	9.42	8.82
Lin 8	(6, 5, 5)	6	(2, 1, 0)	1.36	4.61
Lin 8	(7, 5, 3)	9	(0, 2, 0)	5.46	4.07
Lin 8	(4, 4, 2)	9	(0, 2, 0)	10.08	9.19
Lin 8	(3, 2, 1)	6	(2, 1, 0)	−0.28	16.96

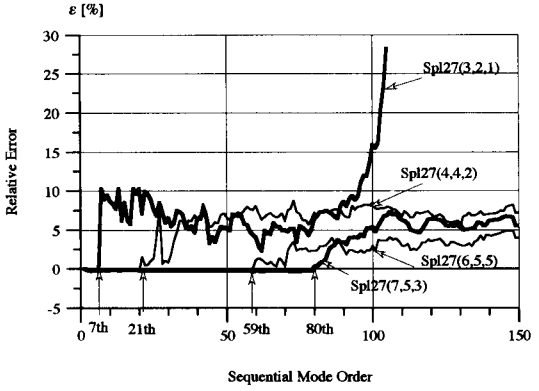

Fig. 7 The relation between relative error, and element division in eigenfrequency computation by Spl 27.

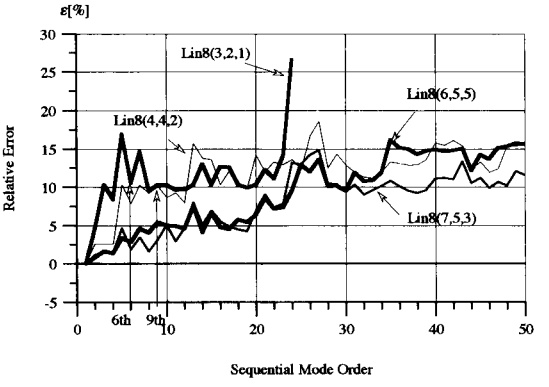

Fig. 8 The relation between relative error, and element division in eigenfrequency computation by Lin 8.

with those by the analytic solution could be found from 1st to (N_0-1)th orders, and N_0th is the first order where modes begin to shift their positions in frequency region. Then, with simple mathematics, it is clear that N_0 coincides with the position where the value of λ/d is equal to 4 in one of the spatial directions.

So, the mechanism obtained in the previous section can successfully be applied to predict the accuracy of eigenanalysis in the three dimensional sound field, and λ/d or N_0 can be used as a guideline to estimate the accuracy of sound field analysis with Spl 27. Here, we tentatively call the "N_0" as "critical order," and below the order the relative error in the eigenanalysis can be estimated to be stable and small, within 1% in this case.

On the contrary, as for Lin 8, the error gradually increases as the number of order increases. The N_0 of Lin 8 is also listed for reference in Table 3 by following the same mode checking procedure applied on Spl 27. These smaller numbers of N_0 compared to those of Spl 27 indicate that the eigenmodes obtained by Lin 8 begin to shift their sequential orders in rather lower frequency region, while Fig. 8 also shows that the shifts do not directly cause critical increases in the errors in the eigenfrequency computations.

To examine more details, another eigenanalysis was carried out using Lin 8 with (14, 10, 6)-division, which has the same degrees of freedom as Spl 27 with (7, 5, 3)-division. Here, Lag 27 with (7, 5, 3)-division was also used for comparison. In the following investigation, the correspondence of the spatial mode orders were confirmed in advance between the modes that have the same sequential numbers. The outline of the correspondence is shown in Table 4 and characteristics of eigenfrequency approximation are given in Fig. 9. In general, the error of Spl 27 is smaller than those of the other two, and its error increases from 1% to 10% at

Table 4 Correspondence of eigenanalysis : analytic solution, FEM by Spl 27 with (7, 5, 3)-division and FEM by Lin 8 with (14, 10, 6)-division.

Analytic Solution			FEM	
No. Analytic	Order (n_x, n_y, n_z)	Frequency [Hz]	Spl 27 ε [%]	Lin 8 ε [%]
1	(0, 0, 0)	0	0.0	0.0
2	(1, 0, 0)	233	0.1	0.2
3	(0, 1, 0)	321	−0.2	0.4
4	(1, 1, 0)	396	−0.1	0.3
5	(2, 0, 0)	466	−0.2	0.8
6	(2, 1 , 0)	566	−0.1	0.7
7	(0, 0, 1)	567	−0.1	1.1
8	(1, 0, 1)	613	−0.1	1.0
9	(0, 2, 0)	642	−0.2	1.7
•	•	•	•	•
75	(6, 1, 1)	1542	−0.4	6.5
76	(2, 3, 2)	1558	−0.3	3.9
77	(3, 4, 1)	1567	−0.3	5.0
78	(4, 4, 0)	1586	−0.3	5.5
79	(4, 2, 2)	1601	−0.3	3.7
80	(0, 5, 0)	1604	10.2	10.3
81	(5, 3, 1)	1613	−0.3	4.2
82	(1, 5, 0)	1621	10.1	10.1
83	(5, 0, 2)	1625	−0.3	5.0
84	(7, 0, 0)	1630	10.2	10.3
85	(6, 2, 1)	1639	−0.3	6.0
•	•	•	•	•
195	(1, 6, 2)	2246	4.3	11.8
196	(5, 6, 0)	2249	4.2	12.0
197	(1, 7, 0)	2257	7.8	17.9
198	(8, 4, 0)	2262	3.8	11.1
199	(9, 2, 1)	2264	5.6	14.1
200	(0, 0, 4)	2267	7.1	17.0
•	•	•	•	•

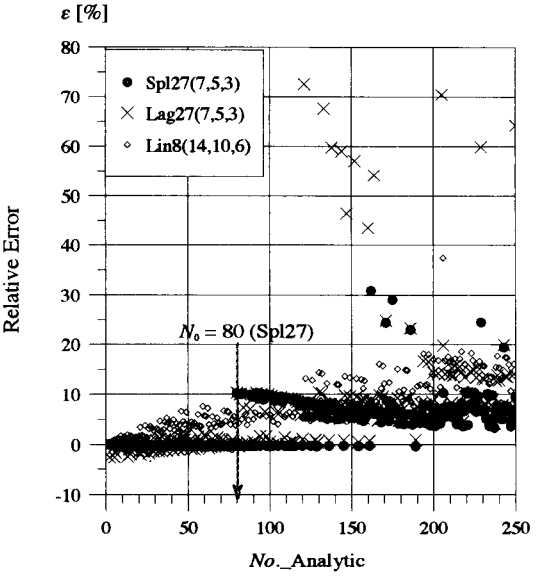

Fig. 9 Comparison of relative error ε in eigenfrequency computations by Lin 8 with (14, 10, 6)-division, Spl 27 with (7, 5, 3)-division and Lag 27 with (7, 5, 3)-division.

the critical order ($N_0=80$) because of the frequency shift of the eigenmode.

6. ESTIMATION OF ACCURACY IN SOUND PRESSURE COMPUTATION

To test the issue given in the previous section, sound pressure computation in a one-dimensional sound field, $1.5\times0.1\times0.1$ [m^3], was carried out using the Linear Acceleration Method to solve the Equation (8) in the time domain.[8] The wall conditions were assumed to be hard and the sound source to be a tone burst with the center frequency of 500 Hz and with 6-waves. The frequency range of the tone burst lies roughly from 350 to 650 Hz.

Here, when the eigenfrequency of the (n_x, 0, 0)th mode equals 650 Hz, the order n_x becomes 5.7. Then, it is safe to estimate N_0 equals 6 in this computation. Since the eigenfrequency $f_{6,0,0}$ equals 680 Hz, the satisfactory accuracy can be expected below the frequency. In this case, λ/d becomes greater than 4.

The results are shown in Fig. 10 and Fig. 11 comparing the element divisions. Figure 10 shows that Spl 27 gives fair agreement if the array of (6, 1, 1)-division, which corresponds with the number of the critical order "6", allocated ; in this case $\lambda/d=4.2>4$. Only a small change can be found if the array is increased to (7, 1, 1)-division ($\lambda/d=4.4>4$), while the agreement becomes worse if the array is reduced to (5, 1, 1)-division ($\lambda/d=3.5<4$). In the latter case, λ/d falls on 4 when the eigenfrequency of a mode becomes 566.7 Hz, which results in about 10% relative error in eigenfrequency approximation.

To the contrary, from the results of Lin 8 in Fig. 11, only small and gradual refinements are observed even if the array is increased from (10, 2, 2)-division ($\lambda/d=3.5$), to (60, 2, 2)-division ($\lambda/d=20.9$). The degrees of freedom for the computation with the array of (10, 2, 2)-division by Lin 8 are the same as those of (5, 1, 1)-division by Spl 27. On the whole, these characteristics of both Spl 27 and Lin 8 agree

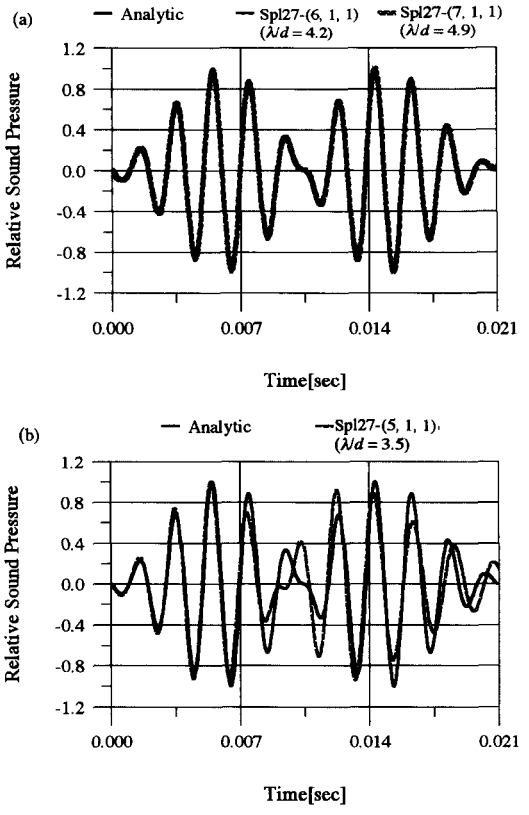

Fig. 10 Comparison of computed sound pressure waveforms; (a) Analytic solution *vs.* FEM by Spl 27 with (6, 1, 1)- and (7, 1, 1)-divisions, (b) Analytic solution *vs.* FEM by Spl 27 with (5, 1, 1)-division.

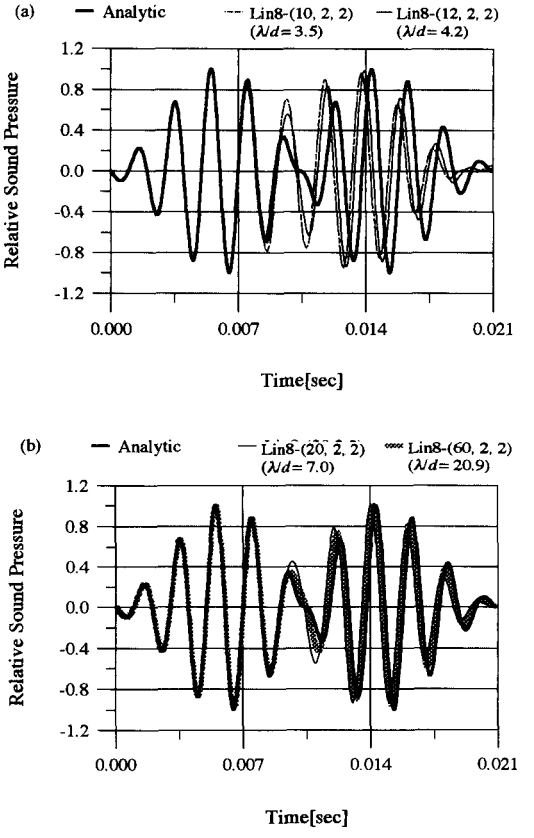

Fig. 11 Comparison of computed sound pressure waveforms; (a) Analytic solution *vs.* FEM by Lin 8 with (10, 2, 2)- and (12, 2, 2)-divisions, (b) Analytic solution *vs.* FEM by Lin 8 with (20, 2, 2)- and (60, 2, 2)- divisions.

with the characteristics given by Fig. 4.

7. CONCLUSIONS

A 27-node isoparametric acoustic finite element using spline polynomial is introduced and its basic characteristics are investigated. From a basic eigenanalysis on a small room using small degrees of freedom, Spl 27 showed the superior approximation to the other elements. Another eigenanalysis revealed the detailed mechanism causing the approximation error, and critical order has been found for Spl 27. Then, systematic error-characteristic curves have been presented for the elements that are expected to give a guideline in applications of the elements on the sound field analysis of three-dimensional rooms, which was confirmed by the results of waveform computations in a one-dimensional sound field. However, above mentioned superior approximation of Spl 27 could be seen only if the guideline was satisfied and further investigations on the applicability of them to three-dimensional sound fields with more complicated conditions would be required.

ACKNOWLEDGEMENT

The authors are indebted to the former graduate students K. Fujii, Y. Takahashi and T. Uchida for the computer implementation of the concepts developed through this research and for cooperative works. This work was supported, in part, by the Grand-in Aid for Science Research (B) 10450214.

SYMBOLS

c: speed of sound

d : nodal distance in a finite element
$f_{i,j,k}$: eigenfrequency of (i, j, k)th mode
f_n : eigenfrequency of nth mode
$f_{n,\mathrm{FEM}}$, $f_{n,\mathrm{Analytic}}$: eigenfrequencies of nth mode obtained by FEM and analytic solution respectively
L_x, L_y, L_z : dimensions of room, x-, y- and z-direction respectively
(l_x, l_y, l_z) : array of element division in x-, y- and z-direction respectively
N_0 : critical order
$\{N\}$: shape function
(n_x, n_y, n_z) : array of spatial mode order in x-, y- and z-direction respectively
n : modal order
p : sound pressure
$\{p\}$: sound pressure vector
T_e : kinetic energy in an element
u_n : normal displacement at Γ_e
$\{u\}$: displacement vector
V_e : potential energy in an element
W_e : work done by external force
Γ_e : elemental boundary of external force
ε : relative error
$\{\phi_n\}$: eigenmode vector
λ : wavelength
ρ : mass density of air
ω : angular frequency
ω_n : eigenfrequency ($\omega_n = 2\pi f_n$)
$\{\ \}$: vector
$\{\ \}_e$: elemental vector
$[\ ]$: matrix
$[\ ]_e$: elemental matrix
$[\ ]^{\mathrm{T}}$: transpose of $[\ ]$

REFERENCES

1) V. Easwaran and A. Craggs, "On further validation and use of the finite element method to room acoustics," J. Sound Vib. **187**, 195–212 (1995).
2) M. Petyt, J. Lea, and G. H. Koopmann, "A finite element method for determining the acoustic mode of irregular shaped cavities," J. Sound Vib. **45**, 495–502 (1976).
3) R. J. Astley and W. Eversman, "The finite element duct eigenvalue problem : An improved formulation with Hermitian elements and No_Flow condensation," J. Sound Vib. **69**, 13–25 (1980).
4) A. Craggs, *Encyclopedia of Acoustics* (John Wiley & Sons, New York, 1997), Chapter 14.
5) T. Watanabe, M. Natori, and T. Oguni, *Numerical Methods, Software by Fortran 77* (Maruzen, Tokyo, 1989), pp. 247–257 (in Japanese).
6) Y. Kagawa, *Sound and Vibration Engineering/ Basics and Application, by Finite Element Method* (Baifukan, Tokyo, 1981), pp. 166–178 (in Japanese).
7) T. Otsuru and H. Yamamoto, "Sound transmission analysis using computational mechanics," J. Acoust. Soc. Jpn. (J) **44**, 293–299 (1988) (in Japanese).
8) T. Otsuru and K. Fujii, "Finite elemental analysis of sound field in rooms with sound absorbing materials," Proc. Inter-Noise 94, 2011–2013 (1994).